Studies of Urohemin I in Aqueous Solution. Thermodynamics of Self-Association and Electronic Properties of Two Species Detected by Proton NMR Spectroscopy

ARTICLE *in* THE JOURNAL OF PHYSICAL CHEMISTRY · NOVEMBER 1984

Impact Factor: 2.78 · DOI: 10.1021/j150667a008

Studies of Urohemin I in Aqueous Solution. Thermodynamics of Self-Association and Electronic Properties of Two Species Detected by Proton NMR Spectroscopy

James D. Satterlee*[1a] and John A. Shelnutt[1b]

Department of Chemistry, University of New Mexico, Albuquerque, New Mexico 87131, and Sandia National Laboratories, Albuquerque, New Mexico 87185 *(Received: February 21, 1984; In Final Form: May 10, 1984)*

The solution chemistry of iron(III) uroporphyrin I chloride (FeURO), or urohemin, has been examined at pH 11–13 by proton NMR spectroscopy at 360 MHz. The hyperfine spectrum is similar to that of iron(III) octaethylporphyrin chloride with pyrrole CH_2^{α} and CH_2^{β} protons appearing substantially downfield (35–45 ppm) and meso protons shifted upfield. Two forms are present in solution and are characterized as monomer and dimer. The dynamics of the monomer–dimer equilibrium are slow on the NMR time scale so that separate sets of resonances are simultaneously observed. The relative concentration of the two forms can be regulated by changing concentration and temperature, with the monomer predominating at high temperatures and low concentrations. An equilibrium quotient has been defined for this process, $Q = [\text{dimer}]/[\text{monomer}]^2$. Q was evaluated as a function of temperature between 0 and 36 °C, with a value at 30 °C of 43.5 M^{-1}. These data yielded estimates of enthalpy (−10.6 ± 1 kcal/mol) and entropy (−27.6 ± 3 cal/(mol °C)) for the dimerization process. Non-Curie temperature dependence is exhibited by the monomer meso proton resonance whereas the dimer meso proton resonance exhibits linear, Curie behavior.

Introduction

Understanding the aqueous solution chemistry of water-soluble ferric porphyrins is of interest for several reasons. Among these are the comparisons which emerge between the properties of porphyrins in water and in lower dielectric media. Also important is the relationship between naked porphyrin chemistry in aqueous solution and heme protein function. This is particularly true in view of the many protein-mediated catalytic reactions directly involving iron porphyrins,[2-6] including ligand binding.[7-13] Recently it has been suggested that free hemin may play a role in malaria chemotherapy,[14] so that understanding the nature of ferric porphyrins in aqueous solution is a prerequisite to quantitative studies of heme–drug interactions.[15]

Metalloporphyrin dimerization in aqueous solution and even in organic solvents is a well-established fact.[16-21] As a consequence, it complicates studies where monomer porphyrin species are desired. Uroporphyrin I and its metal derivatives exhibit an interesting solution chemistry in this respect. Previous work for the free base[13] and several metallouroporphyrins,[7,11,16] with the notable exception of the iron(III) complex, indicates that the extent of aggregation can be regulated and is minimal at concentrations used for Raman and UV–visible spectroscopies.[11]

In this work we show that aqueous urohemin I (ferric uroporphyrin I chloride; FeURO; I)

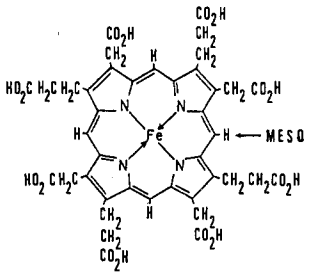

displays solution chemistry in the 10^{-1}–10^{-4} M concentration range that is consistent with a monomer ⇌ dimer equilibrium. The two solution species characterized herein are consistent with a previous study[11] which indicated that FeURO could be forced to dimerize by high salt concentrations, in a manner similar to copper(II) uroporphyrin I (CuURO).[16] Consideration of the dimer hyperfine proton NMR shift pattern indicates that it is not antiferromagnetically coupled and, therefore, it is unlikely to be a μ-oxo-bridged molecule. The pattern of meso proton shifts further indicates that the extent of π-type unpaired spin density delocalization is different for the monomer and the dimer. Finally, equilibrium measurements as a function of temperature have yielded estimates of enthalpy and entropy for this dimerization process.

Experimental Section

Iron(III) uroporphyrin I chloride (FeURO) was purchased from Porphyrin Products (Logan, UT) and purified by column chromatography on Sephadex G-50-40 in 0.1 M base (KOH or NaOH, Fisher). This procedure has previously been shown to remove contaminants responsible for the fluorescence background in Raman studies.[11] The FeURO was precipitated from the column eluent by addition of ethanol and subsequently recrystallized from an aqueous ethanol solution. The resulting proton NMR spectrum revealed no observable impurities.

NMR spectra were obtained at 360 MHz by using Nicolet spectrometers at the Purdue University Biochemical Magnetic

* Address correspondence to this author at the Department of Chemistry, University of New Mexico, Albuquerque, NM 87131.

(1) (a) University of New Mexico, Fellow of the Alfred P. Sloan Foundation, 1983–1985. (b) Sandia National Lbratories.
(2) Hewson, W. D.; Hager, L. P. In "The Porphyrins"; Dolphin, D., Ed.; Academic Press: New York, 1979; Vol. VII, pp 295–332.
(3) Timkovich, R. In "The Porphyrins"; Dolphin, D., Ed.; American Press: New York, 1979; Vol. III, pp 24–2949.
(4) Wilson, D. F.; Erecinska, M. In "The Porphyrins"; Dolphin, D., Academic Press: New York, 1979; Vol. VII, pp 1–70.
(5) Cramer, W. A.; Horton, P. In "The Porphrins"; Dolphin, D., Ed.; Acadmic Press: 1979; Vol VII, pp 71–106.
(6) Giardina, B.; Amiconi, G. *Methods Enzymol.* **1981**, *76*, 417–427.
(7) Shelnutt, J. A. *J. Phys. Chem.* **1983**, *87*, 605–616.
(8) Satterlee, J. D.; LaMar, G. N.; Frye, J. S. *J. Am. Chem. Soc.* **1976**, *98*, 7275–7280.
(9) Satterlee, J. D.; LaMar, G. N.; Bold, T. J. *J. Am. Chem. Soc.* **1977**, *99*, 1088–1093.
(10) Satterlee, J. D.; LaMar, G. N. *J. Am. Chem. Soc.* **1976**, *98*, 2804–2809.
(11) Shelnutt, J. A. *Inorg. Chem.* **1983**, *22*, 2535–2544.
(12) Abbott, E. H.; Rafson, P. A. *J. Am. Chem. Soc.* **1974**, *96*, 7378–7379.
(13) Muazerall D. *Biochemistry* **1965**, *4*, 1801–1810.
(14) Chou, A. C.; Rekka, C.; Fitch, C. D. *Biochemistry* **1980**, *19*, 1543–1549.
(15) Satterlee, J. D.; Constantinidis, I.; Shelnutt, J. A. *Inorg. Chim. Acta* **1983**, *79*, 175–177. Satterlee, J. D.; Constantinidis, I., submitted for publication in *Inorg. Chim. Acta.*
(16) Blumberg, W. E.; Persach, J. J. *J. Biol. Chem.* **1965**, *240*, 870–876.
(17) Viscio, D. B.; LaMar, G. N. *J. Am. Chem. Soc.* **1978**, *100*, 8096–8100.
(18) Mauzerall, D. *J. Phys. Chem.* **1962**, *66*, 2531–2537.
(19) Snyder, R. V.; LaMar, G. N. *J. Am. Chem. Soc.* **1977**, *99*, 7178–7184.
(20) Brown, S. B.; Dean, T. C.; Jones, P. *Biochem. J.* **1970**, *117*, 733–739.
(21) Brown, S. B.; Hazelkonstantinou, H. *Biochim. Biophys. Acta* **1979**, *585*, 143–153.

0022-3654/84/2088-5487$01.50/0

Resonance Laboratory; the Colorado State University Regional NMR Laboratory; or the University of California, Davis, NMR Facility. Samples were contained in 5-mm tubes and spectra were obtained by using 100-ms pulse repetition times with decoupler suppression of the residual water resonance. The residual water reference was used as an internal reference although resonance positions are reported relative to external DSS. Generally 500–15 000 pulses were required for each spectrum. Active temperature regulation was employed and room-temperature spectra were recorded at 24 ± 1 °C. Probe temperature was calibrated with an alcohol NMR thermometer. Samples were dissolved in 99.8% ^2H_2O (Merck) solutions made to the appropriate pH with ^2HCl and NaO^2H (both Merck). Ionic strength was regulated with either KCl or NaCl (Fisher ACS Certified) and pH was monitored with a Beckman Φ70 meter and Fisher combination electrode. Absorption spectra for FeURO characterization and concentration determination were obtained from a Perkin-Elmer Model 330 spectrophotometer using quartz cells of 0.1- or 1.0-cm path.

Equilibrium quotients were obtained by integrating the relative resonance areas of the monomer and dimer peaks and correcting for the fact that the dimer peak areas consist of twice as many protons as do the monomer peak areas for equivalent concentrations of each species. Integrations were carried out in one of three ways: (i) The spectrum was traced onto graph paper and graphically integrated. (ii) Spectra were carefully cut and weighed. (iii) The original spectra were digitized at the average rate of 140 Hz^{-1}, although higher digital resolution was used to define inflection points (see Figure 4). The data were subsequently analyzed in terms of n Lorentzian line shapes by using a Hewlett-Packard 9845T computer. Data output included the following: (a) digitized experimental points used in the calculation; (b) calculated component Lorentzian lines and relative areas of each component; (c) sum of the calculated components. A piece of representative data is shown in Figure 4. The relative areas from all three methods were self-consistent and agreed within 15%.

The equilibrium data were gathered between 0 and 36 °C. To ensure that a monomer ⇌ dimer equilibrium was indeed taking place, without interference from other equilibria, the total integrated area of monomer and dimer resonances should remain constant with temperature even though the relative areas may change. Consequently, the Boltzmann corrected total areas were calculated as a function of temperature and, as shown in Figure 5, remain constant within experimental error over the temperature range for which the equilibrium quotients are calculated.

Results and Discussion

Urohemin Species in Solution at pH 11–13. The proton NMR spectrum of urohemin I in basic solution is shown under varying conditions of temperature and concentration in Figures 1 and 2. These spectra are characteristic of ferric porphyrins[8-10,22,23] for which large shifts are caused by the hyperfine fields of the iron-centered paramagnetism. Two mechanisms may convey the effect of this paramagnetism to the protons at the porphyry periphery, the contact and pseudocontact (dipolar) interactions. The total observed shift for each proton is then the sum of diamagnetic, contact, and dipolar shifts (eq 1 and 2). The parameters in these

$$(\Delta H/H)_{obsd} = (\Delta H/H)_{dia} + (\Delta H/H)_{dip} + (\Delta H/H)_{com} \quad (1)$$

$$\left(\frac{\Delta H}{H}\right)_{obsd} = \left(\frac{\Delta H}{H}\right)_{dia} - \frac{\beta^2 S(S+1)}{9kT}(g_\parallel^2 - g_\perp^2)\langle(3\cos^2\theta - 1)r^{-3}\rangle - Ag\beta S(S+1)(3\gamma_N hkT)^{-1} \quad (2)$$

equations have been defined elsewhere.[22-24] The second equation is a simplified form of the more general case[23,24] and explicitly neglects second-order Zeeman contributions. It assumes a single populated spin level and effective axial symmetry, both valid at least for monomeric urohemin I.[22-24]

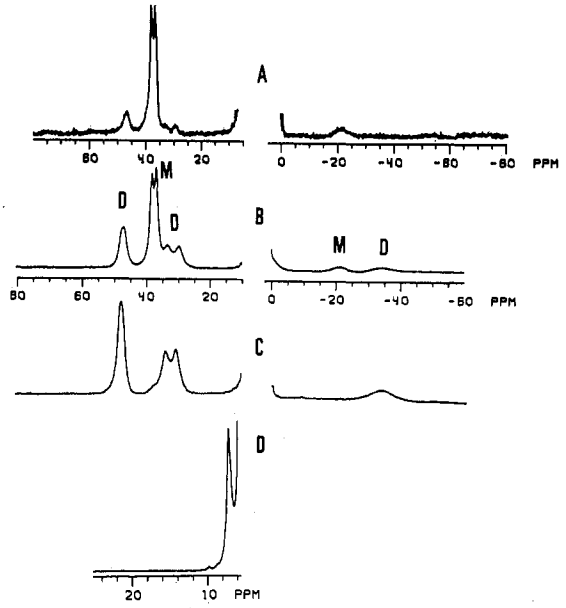

Figure 1. (A) 7.5 × 10^{-4} M FeURO, pH 13.5, 24 °C, showing predominantly the monomer resonances; (B) 10.8 × 10^{-3} M FeURO, pH 13.5, 24 °C, showing both monomer and dimer resonances; (C) 10.8 × 10^{-3} M FeURO, pH 13.5, 24 °C, in saturated KCl solution showing the dimer resonances; (D) 10.8 × 10^{-3} M FeURO, pH 5.8, 22 °C, showing the β-CH_2 propionic acid proton resonance near 9 ppm. Note the different scales in A, B–C, and D. Meso protons appear upfield; α-CH_2 appear downfield and are labeled M (=monomer) or D (=dimer).

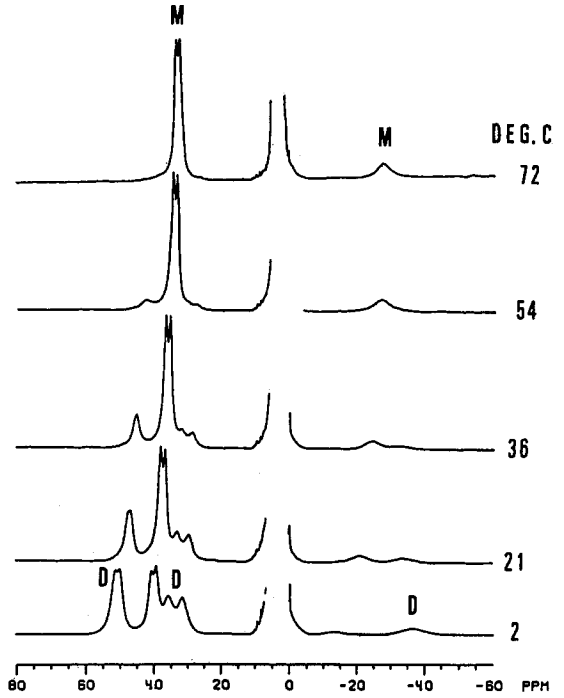

Figure 2. Effect of temperature on the hyperfine spectrum of 10.8 × 10^{-3} M FeURO, pH 13.5, showing the predominance of the monomer at higher temperatures and significant dimer formation at lower temperatures. Equilibrium quotients described in the text were extracted from data such as those presented in this figure.

The proton spectrum of 10^{-2} M FeURO shown in Figure 1B displays eight resolved hyperfine resonances outside the diamagnetic region (0–10 ppm). The diamagnetic area is excluded from these figures because it shows only the broad, residual water resonance. Changing the concentration (Figure 1A,B) or satu-

(22) LaMar, G. N. In "Biological Applications of Magnetic Resonance"; Shulman, R. G., Ed.; Academic Press: New York, 1981; pp 122–162.
(23) Jessen, J. P. In "NMR in Paramagnetic Molecules"; LaMar, G. N., Horrocks, W. D., Holm, R. H., Eds.; Academic Press: New York, 1973; pp 1–52.
(24) LaMar, G. N.; Walker, F. A. In "The Porphyrins"; Dolphin, D., Ed.; Academic Press: New York, 1979; Vol. IV, pp 61–157.

TABLE I: Observed Proton Hyperfine Shifts for the Monomer and Dimer of FeURO in Comparison with Other Ferric Porphyrins

				shift,[a] ppm				
				pyrrole substituents				
compd[b]	solv	pH	temp[c]	CH_2^α	CH_2^β	CH_3^β	meso[d]	ref
FeUROCl (monomer)	D_2O	11.8	30	+37.2, 35.9	<8.5		−23.5	this work
OEPFeCl	$CDCl_3$		29	+43.1, 39.5		+6.65	−55	30, 24
DPDMEFeF			35	+26			−35	44, 24
DPDMEFeCl	$CDCl_3$		35	+37, 35, 31			−57	44, 24
MPDMEFeCl	$CDCl_3$		25	+36, 35			−43	
PPFeCl	Me_2SO-d_6		32	+36			−50	46, 24
$PPFe(Me_2SO)_2^+$	Me_2SO-d_6		32	+41			+40	46, 24
$DPFe(Me_2SO)_2^+$	Me_2SO-d_6		32	+41, 38			+40	46, 24
$MPFe(Me_2SO)_2^+$	Me_2SO-d_6		25	+46		+5.7	+40, 39	24
FeUROCl (dimer)	D_2O	11.8	30	+45.8, 32.4, 29.1		+5.7	−33.6	this work
$(OEPFe)_2O$	$CDCl_3$		29	+6.06, 5.1		+1.75	+5.5	30, 24
$(PPDMEFe)_2O$	$CDCl_3$		29	+6.1, 6.2			+6.5[d]	45, 24
$(DPDMEFe)_2O$	$CDCl_3$		29	+6.4			+6.5[d]	45, 24

[a] Observed shift for FeURO referenced internally to the residual water resonance, subsequently reported relative to external DSS; + indicates shift downfield from DSS; − indicates shift upfield from DSS. Shifts for porphyrins in $CDCl_3$ or Me_2SO are referenced to Me_4Si. [b] Abbreviations: DPDME = deuteroporphyrin in dimethyl ester; PPDME = protoporphyrin IX dimethyl ester; MPFeDME = mesoporphyrin dimethyl ester; OEP = octaethylprophyrin; URO = uroporphyrin I; Me_2SO-d_6 = perdeuterated dimethyl sulfoxide. [c] In °C. [d] ±1.5 ppm.

rating the FeURO solution with salt (NaCl, KCl, Figure 1c) alters the spectrum systematically. The peaks are numbered 1–8 beginning at the left. At low concentrations resonances 3, 4, and 7 predominate (M). At higher concentration or upon salt addition, resonances 1, 2, 5, 6, and 8 predominate (D). Similarly, the temperature dependence of FeURO shown in Figure 2 indicates that the species typified by resonaces, 3, 4, and 7 is favored at higher temperatures whereas the species displaying resonances 1, 2, 5, 6, and 8 predominates at lower temperature. These results indicate that, at the resolution offered by NMR, only two interconverting forms of FeURO are observed. This observation is valid for highly basic solutions at pHs greater than 9.5 and is consistent with the established view that water-soluble metalloporphyrins may undergo a dimerization equilibrium.[13,17,18–21,25–27]

It will be demonstrated later that the temperature-dependent interconversion of the two sets of resonances can be interpreted in terms of a monomer–dimer equilibrium. Assuming this point of view we may attribute each set of resonances to the monomer or dimer. At lower concentrations and higher temperatures the monomer should predominate (resonances 3, 4, and 7). At higher concentrations and lower temperature the dimer should prevail (resonances 1, 2, 5, 6, and 8). Substantiation for this equilibrium picture comes from earlier work by Blumberg and Peisach[17] on copper uroporphyrin III and in comparison with a companion article.[28] In the earlier EPR study it was concluded that high CuURO concentrations or addition of salt caused dimer formation.[17] Subsequently, in a recent study of several metallouroporphyrins,[28] we have shown that high salt concentrations cause changes in the Raman and absorption spectra of all the metallouroporphyrin solutions similar to those changes induced in CuURO solution. From these results we can conclude that FeURO in a saturated salt solution is essentially dimeric. Therefore, its proton NMR spectrum (Figure 1D) reinforces the assignment of the dimer species to resonances 1, 2, 5, 6, and 8.

Resonance Assignments. In order to assign the proton resonances of the FeURO monomer and dimer, we made use of relative peak areas obtained by integration and comparison with spectra of similar ferric porphyrins (Table I). Consider first the monomer. In the uroporphyrin structure there are four types of protons: eight each of the propionic acid side chain CH_2^α and CH_2^β; eight acetic acid substituents CH_2^α; and four at the porphyrin meso positions. A related structure is ferric octaethylporphyrin (FeOEP) whose assignments[24] are shown in Table I. FeOEP is an organic-solvent-soluble porphyrin with ethyl groups substituted at the eight pyrrole positions. The common features with FeURO are the 16 CH_2^α pyrrole substituents and the four meso protons.

In general, the shift pattern of the monomer (Table I) suggests strongly that it is best visualized as a high-spin ferric porphyrin. The relative intensities of the three resolved resonances in FeURO monomer are 4:4:1 for resonances 3:4:7. The broad upfield resonance is assigned to the meso position protons and is characteristic of a high-spin ferric porphyrin as shown by entries 2–6 in Table I. This assignment is based on many types of ferric porphyrin spectra[22–24] and the relative integrations. The fact that this meso resonance does not lie as far upfield as the other chloro complexes in Table I is significant and will be discussed further on. Similarly, the assignment of the pyrrole CH_2^α protons comes from the characteristic shift position of these types of protons and their intensities relative to the meso proton resonance. The appearance of a doublet for the CH_2^α protons is consistent with the FeOEP spectrum where the doublet is due to diastereotopism. However, we cannot unambiguously assign this doublet to diastereotopism, where acetic and propionic acid pyrrole CH_2^α groups have the same observed shifts within the spectrometer resolution. An alternative explanation is that the diastereotopism is not resolved within each peak and that two resonances (3, 4) are attributable to the two different types of pyrrole substituents (acetic vs. propionic). However, on the basis of the FeOEP spectrum and the fact that at higher temperatures the two peaks of the doublet tend toward coalescence (the shift difference is 1.3 ppm at 2 °C whereas at 72 °C the difference is only 1.0 ppm and the linear regression intercepts at $T^{-1} = 0$ differ only by 0.7 ppm), we consider the former explanation more likely. The coalescence is accounted for by increased side-chain mobility with higher temperature which tends to average the environments of the two diastereotopic protons as the temperature increases. The FeURO propionic substituent CH_2^β is in a position relative to the heme comparable to the FeOEP CH_3^β substituent. Similarly, in FeURO monomer CH_2^β is found well upfield relative to the CH_2^α and under the residual water resonance at pH values greater than 9.5. Below this pH the CH_2^β protons are observed because they shift downfield, away from the residual H^2HO peak (Figure 1D) and are confirmed by integration.

For the set of resonances (1, 2, 5, 6, 8) that we have ascribed to the FeURO dimer, the only certain assignment is of the meso proton resonance, upfield at −33.6 ppm (peak 8). This comes from comparison with other ferric porphyrin shifts, its line width comparable to the FeURO monomer meso resonance, and its integrated intensity which shows equal relative ratios for resonances 1, 2, 5, 6, and 8 (cf. Figure 4). The downfield dimer resonances with shifts of 45.8 (two peaks), 32.4, and 29.1 ppm at 30 °C are assignable to pyrrole CH_2^α substituents by the same

(25) Brown, S. B.; Hazelkonstantinou, H.; Herries, D. G. *Biochim. Biophys. Acta* **1976**, *539*, 338–351.
(26) Goff, H.; Morgan, L. O. *Inorg. Chem.* **1976**, *15*, 2062–2068.
(27) White, W. I. In "The Porphyrins"; Dolphin, D., Ed.; Academic Press: New York, 1979; Vol. V, pp 303–339.
(28) Shelnutt, J. A.; Dobry, M. M.; Satterlee, J. D. *J. Phys. Chem.* **1984**, *88*, 4980–4987.

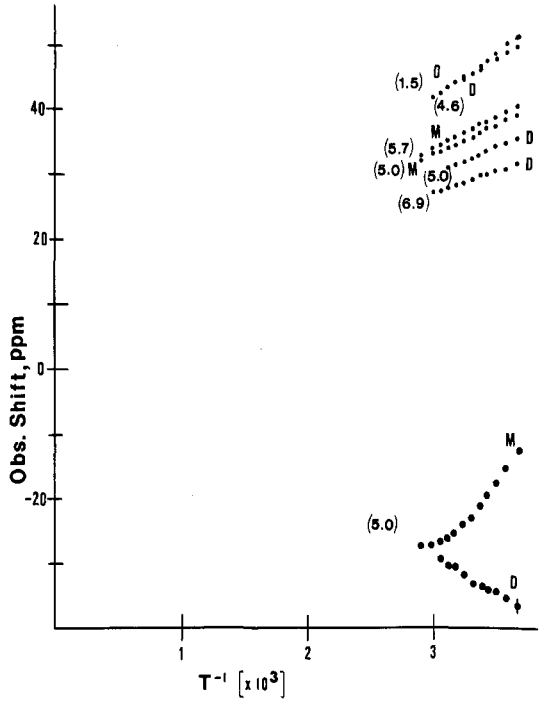

Figure 3. Curie plot of the FeURO (10.8×10^{-3} M, pH 13.5) variable-temperature data. M = monomer, D = dimer peaks, and the numbers in parentheses represent the y intercept obtained by linear regression. All peaks behave according to the Curie law (eq 1 and 2) with correlation coefficients greater than 0.996 except the monomer meso resonance.

criteria as before. At this point any further attempt at assigning the resonances would be too speculative. What we can state for certain is that the dimer shifts for ferric urohemin I are not characteristic of a strongly antiferromagnetically coupled system. That rules out the characterization of the dimer as one which contains a μ-oxo bridge. This is illustrated by comparing the last four entries of Table I. It is clear that the FeURO dimer shifts are much larger than those published for common μ-oxo dimer ferric porphyrins. These NMR data are consistent with the concept of π–π complex formation,[28,29] with each molecule in the complex being essentially a high-spin ferric porphyrin. Although a weakly coupled μ-hydroxo dimer[25] cannot be excluded for ferric uroporphyrin I, it is unlikely for several other metallouroporphyrins that exhibit similar monomer–dimer equilibria and aggregation-induced spectral changes.[28,29]

Variable-Temperature Data. The behavior of the observed hyperfine shifts as a function of temperature are presented in Figure 3 in the format of the Curie law described by eq 2. Except for the FeURO monomer meso resonance, all of the observed proton resonances display Curie behavior with extrapolated intercepts of $T^{-1} = 0$ in the diamagnetic region.[22] The behavior of the meso proton resonance is extremely anti-Curie at lower temperatures, but shows a turn to more Curie-like behavior at higher temperatures.

These data may be interpreted if one makes the reasonable assumption that the observed shifts in the high-spin FeURO monomer and dimer originate in the same mechanisms of electron spin density delocalization as in the synthetic high-spin ferric porphyrins.[23,24,30,31] The similarity of the FeURO shifts observed here to those of FeOEP and other ferric porphyrins indicates a consistent pattern with substantially downfield CH_2^{α} shifts, substantially upfield meso resonance shifts, and slight downfield pyrrole β-proton shifts. This pattern has been interpreted as originating in a mechanism wherein the hyperfine shift is due primarily (>85%) to the contact shift.[24,30,31]

The pattern of covalent spin delocalization has been shown to involve both σ- and π-type porphyrin molecular orbitals.[24] Appearance of spin density at the pyrrole carbons is primarily due to spin density transfer through the σ orbital network whereas at the meso positions a π symmetry orbital contains the unpaired spin density.[24] The large upfield meso shifts observed for both the FeURO monomer and dimer are consistent with significant metal-to-ligand back-bonding of the type $Fe(d_{xz},d_{yz}) \rightarrow Por(4e_g\pi^*)$. The porphyrin $4e_g\pi^*$ orbital has the largest coefficients at the meso positions.[32,33] The alternative, ligand-to-metal covalency of the type $Por(3e_g\pi) \rightarrow Fe(d_{xz},d_{yz})$ cannot alone account for the large observed meso shift because the $3e_g\pi$ porphyrin orbital exhibits nodes at all meso positions.[32,33]

Equation 2 indicates that all observed hyperfine shifts must extrapolate to their diamagnetic positions as the temperature approaches infinity. The non-Curie behavior observed for the monomer meso proton resonance must be due to a temperature-dependent process superimposed on normal Curie behavior.

Two possibilities seem likely to account for this non-Curie behavior. In one, temperature-dependent covalency in the $Fe(d_{xz},d_{yz}) \rightarrow Por(4e_g\pi^*)$ back-bonding would be the source of the anomalous temperature dependence. Such a model is related to the metal–ligand covalency picture developed for tris(chelate) complexes of various transition metals by LaMar and van Hecke.[34-36] This model could lead to detectable temperature-dependent effects in the absorption spectrum, but need not if unpaired spin delocalization and covalency in the urohemin monomer consists of synergistic bonding between iron-centered d orbitals and porphyrin $4e_g\pi^*$ *and* $3e_g\pi$ orbitals.

A less esoteric, and we consider more likely, origin of deviations from Curie behavior is a ligation equilibrium between five- and six-coordinate urohemin monomer forms. The data of Table I and ref 37 reveal that five-coordinate and six-coordinate ferric porphyrins exhibit similar photon shifts for identical pyrrole substituents on the porphyrin periphery. For example, the methylene proton hyperfine shifts observed for each of these species occur in a small range centered about 35 ppm downfield. The pyrrole substituents are essentially insensitive to the extent of axial ligation in these ferric porphyrins.

However, Table I demonstrates that meso proton resonances are more sensitive to axial ligation state. As shown before for derivatives of protohemin IX,[24,37] the results collected in Table I indicate that for five-coordinate complexes (OEPFeCl; DPDMEFeCl,F; MPDMEFeCl; PPFeCl) tyical meso proton shifts are observed between 35 and 57 ppm *upfield* from Me_4Si. For six-coordinate complexes ($PPFe(Me_2SO)_2^+$; $DPFe(Me_2SO)_2^+$; $MPFe(Me_2SO)_2^+$) the observed meso proton hyperfine shifts appear 39–40 ppm *downfield* from Me_4Si. The downfield bias of six-coordinate high-spin ferric porphyrins provides a mechanism to account for our observation of a more downfield meso proton resonance in monomer urohemin than in the dimer. A kinetically rapid axial ligation process involving only a small fraction of the total monomer population at any given time, indicating a low equilibrium constant for six-coordination, could account for the observed downfield bias at lower temperatures and the anomalous temperature dependence of the meso proton resonance. Thus, at lower temperatures an increased downfield shift for the meso resonance (Figure 3) is consistent with the normal temperature dependence of an equilibrium constant indicating a greater fraction of six-coordinate monomer, thereby demonstrating an observed

(29) Shelnutt, J. A. *J. Phys. Chem.* **1984**, *88*, 4988–4992.
(30) LaMar, G. N.; Eaton, G. R.; Holm, R. H.; Walker, F. A. *J. Am. Chem. Soc.* **1973**, *95*, 63–74.
(31) Walker, F. A.; LaMar, G. N. *Ann. N.Y. Acad. Sci.* **1973**, *206*, 328–348.
(32) Zerner, M.; Gouterman, M.; Kobayashi, H. *Theor. Chim. Acta* **1966**, *6*, 363–400.
(33) Longuet-Higgins, H. C.; Rector, C. W.; Platt, J. R. *J. Chem. Phys.* **1950**, *18*, 1174.
(34) LaMar, G. N.; van Hecke, G. R. *J. Am. Chem. Soc.* **1970**, *92*, 3021–3028.
(35) LaMar, G. N.; van Hecke, G. R. *J. Am. Chem. Soc.* **1972**, *94*, 9049–9055.
(36) LaMar, G. N.; van Hecke, G. R. *J. Magn. Reson.* **1971**, *4*, 384–391.
(37) Abraham, R. J.; Barnett, G. H.; Bretschneider; E. S.; Smith, K. M. *Tetrahedron* **1973**, *29*, 553–560.
(38) Petrekis, L.; Dickson, F. E. *J. Mol. Struct.* **1972**, *11*, 361–369.

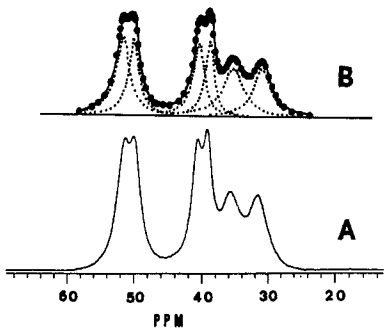

Figure 4. Integration of the actual downfield hyperfine spectrum (A) for the 2 °C spectrum carried out by using a Lorentzian line-fitting program (B). The digitized data points taken from the experimental spectrum are shown by large filled circles. The dotted lines show the calculated component peaks, and the solid line represents the sum of the Lorentzian components.

TABLE II: Calculated Equilibrium Quotients as a Function of Temperature for the FeURO Monomer–Dimer Interconvolution

temp, °C	Q, M^{-1}	temp, °C	Q, M^{-1}
1.5	265	18	83.6
8	173	24	63.5
14	109	30	43.5
		36	30.5

[a] Q estimated accuracy ±15%.

meso shift much less than the dimer. Similarly, increasing temperature causes decreasing values for the equilibrium constant and in the limit, behavior by the urohemin monomer which is typical of five-coordinate species, like the dimer. This is the observed behavior.

The strict Curie dependence of the dimer meso proton resonance and its more upfield shift indicate that the dimer is best considered to be five-coordinate throughout the temperature range that we have examined. In view of the proposed face-to-face dimer structure (vide infra) only one of the two possible axial coordination sites is available to H_2O, or OH^- for ligation purposes.

Finally, the resonances that follow the Curie law show no detectable curvature as indicated by the linear regression correlation coefficients (all greater than 0.999) which accompany the intercepts at $T^{-1} = 0$, displayed in Figure 3. This makes it impossible to evaluate zero-field splitting induced pseudocontact (dipolar) shifts for FeURO. We hasten to point out that over the temperature range accessible to us for these studies, existing curvature may be so slight as to be undetectable. One cannot justifiably conclude the nonexistence of dipolar shifts. Curvature could become apparent over a broader temperature range.

Equilibrium. In view of the relative assignments of the two species in solution as monomer and dimer, the temperature dependence of the relative peak intensities has been interpreted in terms of the equilibrium

$$2\text{monomer} \rightleftharpoons \text{dimer} \quad (3)$$

$$Q = [\text{dimer}]/[\text{monomer}]^2 \quad (4)$$

where Q is an equilibrium quotient for association. The relative peak areas were evaluated by three methods as described in the Experimental Section. The three methods independently yielded the same results. An indication of the degree of accuracy of these integrations is shown in Figure 4, where one set of experimental data is shown with its analysis by six Lorentzian lines. This figure shows that the calculated spectrum from the six-line approximation is, indeed, very good.

Equilibrium quotients were calculated as described in the Experimental Section and are presented in Table II. Figure 5 gives ln Q as a function of reciprocal temperature and shows that the total integrated area of the CH_2^{α} (monomer + dimer) resonances remains constant between 2 and 36 °C, within the estimated experimental error (15%). This indicates that the two-species equilibrium described by eq 3 and 4 is valid over this

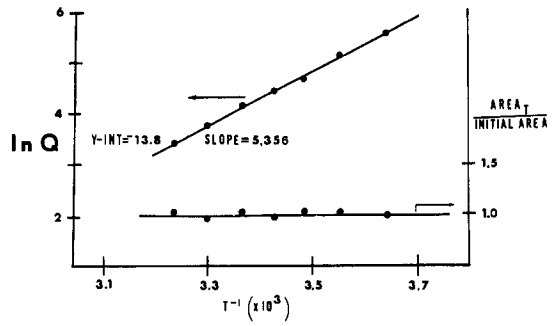

Figure 5. Plot of ln Q (left axis) and the sum of the monomer and dimer resonance areas (right axis) against T^{-1}. The ln Q plot yields a slope and intercept from which ΔH and ΔS are calculated. Data were analyzed by linear regression and the correlation coefficient is 0.9989. The right-axis data indicate the validity of Q over the temperature range chosen by showing that the total area is preserved so that area lost by the dimer upon increasing temperature appears in the monomer resonances.

temperature range. At temperatures above 40 °C the amount of dimer present in solution is too small to accurately integrate its peak areas. Apparent enthalpy (−10.6 ± 1 kcal/mol) and entropy (−27.6 eu) values were evaluated from the slope and y intercept of the ln Q vs. T^{-1} plot by using eq 5.[8,37]

$$\Delta H - T\Delta S = -RT \ln Q \quad (5)$$

The negative ΔS value is expected for an associative process, although the values of the enthalpy and entropy are somewhat larger than those reported for the π–π dimerization of other porphyrins.[17,37-39] The differences can likely be attributed to the differences in solvent systems between this work and that reported elsewhere (aqueous vs. organic), in that it is reasonable to expect the driving force for dimerization of these porphyrins to be higher in the higher dielectric medium.

Conclusions

The data presented in this work indicate that the aqueous solution chemistry of FeURO is interpretable in terms of a monomer ⇌ dimer equilibrium in the millimolar concentration range at pH values greater than 9.5. This makes it possible to regulate the species available for study by adjusting concentration, temperature, and ionic strength. Direct comparisons are then possible between Raman and UV–visible studies, where the concentration range is much lower (10^{-2}–10^{-7} M), and NMR, where practical concentrations must be greater than 10^{-4} M. The FeURO is also interesting because the dynamics of the equilibrium are slow enough so that distinct spectra are observable for each species. A similar state of affairs is observed for the heme undecapeptide, where separate sets of resonances characteristic of monomer and dimer forms have been observed.[40]

Although our present inability to make unambiguous assignments in the dimer spectrum precludes a detailed analysis of the dimer structure, we can point out that a face-to-face structure is most consistent with the observed line widths of the dimer resonances. Unlike data for other iron porphyrins[17,19,40-44] the FeURO dimer spectrum presented here shows no variable line widths within the dimer over the temperature range of Figure 2 (compare resonances 1, 2, 5, and 6). Moreover, the line widths of the resolved dimer resonances are less than a factor of 2 greater

(39) Boyd, P. D. W.; Smith, T. D.; Price, J. H.; Pilbrow, J. R. *J. Chem. Phys.* **1972**, *56*, 1253–1265.
(40) Scatterlee, J. D. *Inorg. Chim. Acta* **1983**, *79*, 195–197.
(41) Viscio, D. B.; LaMar, G. N. *J. Am. Chem. Soc.* **1978**, *100*, 8092–8096.
(42) LaMar, G. N.; Satterlee, J. R.; Snyder, R. V. *J. Am. Chem. Soc.* **1974**, *96*, 7137–7138.
(43) Fulton, G. P.; LaMar, G. N. *J. Am. Chem. Soc.* **1976**, *98*, 2119–2125.
(44) LaMar, G. N.; Viscio, D. B. *J. Am. Chem. Soc.* **1974**, *96*, 7354–7355.
(45) Caughey, W. S.; Johnson, L. R. *J. Chem. Soc. D* **1969**, 1362–1363.
(46) Caughey, W. S.; Barlow, C. H.; O'Keefe, D. H.; O'Toole, M. C. *Ann. N.Y. Acad. Sci.* **1973**, *206*, 296–308.
(47) Kurland, R. J.; Little, R. G.; Davis, D. G.; Ho, C. *Biochemistry* **1971**, *10*, 2237–2242.

than the line widths exhibited by the monomer resonances. From these data we may conclude that differential line broadening from intermolecular paramagnetic dipolar relaxation[17,19,24,48] is undetectable in our spectra. This implies a symmetrical structure for a tight $\pi-\pi$ dimer because the alternative structure in which the dimer is characterized by large interplane distances, regardless of its structure, is inconsistent with the large changes observed in the absorption spectrum that accompany dimer formation as discussed elsewhere.[28,29] However, the observation of a single meso resonance for the dimer argues for a symmetrical face-to-face disposition of the two porphyrin planes.

Finally, we have employed an interpretation here which involves only monomer and dimer. This is the simpliest interpretation that fits the available data and is consistent with many other studies.[13,18,21,25,27] Whereas our data could be interpreted by employing the view that higher order aggregates are present, we believe this unnecessary. Moreover, even at proton frequencies of 470 MHz we have not been successful in resolving more than a single set of resonances attributable to the dimer. Indeed, if equilibrium-dependent higher aggregates are present with shifts identical with those of the dimer, significant line broadening due to these higher molecular weight species should be observed, and, more importantly, the line broadening should be concentration dependent. As discussed in the text, we have observed neither of these effects.

Acknowledgment. This work was funded by grants from the Sandia National Laboratories (SURP) and the National Institutes of Health (AM 30912) to J.D.S., and by the U.S. Department of Energy contract DE-AC04-76-DP00789 (J.A.S.). Use of the Purdue University Biochemical Magnetic Resonance Laboratory was made possible by support from the National Institutes of Health, Division of Research Resources RR 01077. We thank Prof. John Markley and Dr. Milo Westler for providing such a user-oriented facility. The Colorado State University Rocky Mountain Regional NMR Laboratory was made available for our use by support from the National Science Foundation, grant CHE 8208821. We also thank one of the reviewers for comments about the anomalous temperature dependence.

Registry No. FeUROCl, 92284-96-3.

(48) Budd, D. L.; LaMar, G. N.; Smith, K. M.; Nayyir-Mazhir, R. *J. Am. Chem. Soc.* **1979**, *101*, 6091-6096.

Search for the Rydberg States of Transition-Metal Complexes. Hexafluoroacetylacetonates

L. S. Lussier, C. Sandorfy,*

Département de Chimie, Université de Montréal, Montreal, Québec, Canada H3C 3V1

A. Goursot, E. Penigault,

Laboratoire de Photochimie Générale, Equipe de Rechereche Associée au CNRS No. 386, Ecole Nationale Supérieure de Chimie, 68093 Mulhouse Cedex, France

and J. Weber

Laboratoire de Chimie Théorique Appliquée, Université de Genève, CH-1211 Geneve 4, Switzerland
(Received: March 1, 1984)

The far-ultraviolet spectra of transition-metal complexes contain intense absorption bands, most of which could be assigned to charge-transfer transitions. It is shown, however, that a number of strong Rydberg bands must exist which are likely to fall in the same region of the spectrum. The vapor-phase vacuum-UV spectra up to about 72 000 cm^{-1} of the hexafluoroacetylacetonate complexes of Al(III), Sc(III), V(III), Cr(III), Mn(III), Fe(III), and Cu(II) were determined. Qualitative arguments based on estimated Rydberg values, as well as semiquantitative SCF Xα calculations, indicate that Rydberg excitations do contribute to the features observed at energies higher than 40 000–50 000 cm^{-1}, depending on the complex. The present results suggest that it is essential to take into account Rydberg states when interpreting the 50 000–70 000-cm^{-1} region of the far-UV absorption spectra of coordination compounds.

Introduction

The visible and near-ultraviolet parts of the electronic spectra of transition-metal complexes are, in general, well understood. The weak, characteristics d–d transitions, which are found in the visible, received by far the most attention. The much more intense bands which follow at higher frequency are usually interpreted in terms of metal to ligand or ligand to metal charge transfer or intraligand transitions. Early attempts to locate Rydberg bands in the far-ultraviolet region were reviewed by Robin.[1] The difficulty of measuring the spectra of transition-metal complexes in the vapor phase poses a problem. A significant number of transition-metal complexes has, however, a sufficiently high vapor pressure for measuring UV and photoelectron spectra. Among these we selected the hexafluoroacetylacetonate (hfaa) complexes and succeeded in measuring the vapor-phase spectra, up to about 72 000 cm^{-1} (or 140 nm), of the $(hfaa)_3$ complexes of Sc(III), V(III), Cr(III), Mn(III), and Fe(III) and the $(hfaa)_2$ complex of Cu(II). For the sake of comparison, the spectrum of $Al^{III}(hfaa)_3$ was also determined as well as that of hexafluoroacetylacetone itself.

In order to assign the main features of the spectra and to have a better knowledge of their charge transfer (CT) vs. Rydberg origin, reliable calculations of the excited states of these complexes were required. We have chosen to this end the multiple-scattering (MS) Xα molecular orbital (MO) model, which has been shown in the past few years to give a realistic description of the electronic structure of coordination compounds.[2-6] Indeed, Xα predictions

(1) Robin, M. B. "Higher Excited States of Polyatomic Molecules"; Academic Press: New York, 1974; Vol. II, Chapter VIIB.

(2) Weber, J.; Geoffroy, M.; Goursot, Penigault, E. *J. Am. Chem. Soc.* **1978**, *10*, 3995.

(3) Weber, J.; Goursot, A.; Penigault, E.; Ammeter, J. H.; Bachmann, J. *J. Am. Chem. Soc.* **1982**, *104*, 1491.

0022-3654/84/2088-5492$01.50/0